

Analysis of Localized Bioimpedance from Healthy Young Adults During Various Vocal Folds Activities using Cole-impedance Model Representations

Todd J. Freeborn^a, Memorie Gosa^b

^a*Department of Electrical and Computer Engineering, The University of Alabama,
Tuscaloosa, AL, USA, 35487*

^b*Department of Communicative Disorders, The University of Alabama, Tuscaloosa, AL,
USA, 35487*

Abstract

The passive electrical properties of a biological tissue, referred to as the tissue bioimpedance, are related to the underlying tissue physiology. These measures have not been explored as a method to assess the health of vocal fold tissues by detecting vocal fold pathologies, which requires exploring differences between healthy and pathological tissues as well as methods to represent and analyze tissue impedances (which motivates this work). *Objective:* To determine if there are statistically significant differences in Cole-impedance model parameters that represent averaged bioimpedance measurements of localized neck tissues during four vocal folds activities (adducted, abducted, voicing). *Approach:* Tissue bioimpedance was collected from healthy young adults ($N = 10$) in four vocal fold states with averaged datasets reduced to their Cole-impedance model representations (R_∞ , R_1 , C , α) using a particle swarm optimization approach. *Main Result:* The Cole-impedance model does well represent the collected bioimpedance datasets, but no statistically significant differences in the identified Cole-model parameters of the averaged localized bioimpedance datasets across four vocal folds activities were observed. *Significance:* Averaged electrical tissue properties may not be sensitive to variations from vocal folds activity. Therefore, localized tissue bioimpedance may be an alternative

Email address: tjfreeborn1@eng.ua.edu (Todd J. Freeborn)

technique to assess vocal fold tissue health that does not require phonation.

Keywords: Bioimpedance, Cole-impedance model, Vocal Folds, Adduction, Abduction, Voicing

1. Introduction

Dysphonia refers to any difficulty with the voice including perceived abnormalities in the vocal quality indicators of roughness, breathiness, strain, pitch, nasality, and/or loudness that impacts the individual’s ability to communicate or reduces their voice-related quality of life [1, 2]. It is perceptual manifestation of observable changes to the structure or function of the larynx. The causes of dysphonia vary from acute laryngitis to more concerning benign neoplasms and malignancies [3, 4]. In terms of prevalence, a recent study estimated that 1.7% of the adult population in the United States of America are currently diagnosed with dysphonia [3, 4].

Diagnosis of dysphonia typically involves a thorough review of medical history, a perceptual assessment of the individual’s voice quality, acoustic measures, and direct visualization of the larynx [5]. If there are detectable deviations in auditory perceptual measures of vocal quality, then a thorough and detailed diagnostic laryngeal endoscopic evaluation is required [6]. Currently, the laryngeal endoscopic evaluation is the only diagnostic measure that can definitively identify the presence of laryngeal pathology as a contributing factor to dysphonia. It involves the passing of a rigid or flexible endoscope through the mouth or nose for direct visualization of the larynx. Flexible endoscopy is invasive and uncomfortable, often requiring the use of local anesthetic for compliance [7]. Additionally it has been shown to cause significant changes to heart rate, blood pressure, and oxygen saturations in pediatric and adult populations [8, 9]. Transnasal flexible endoscopy is preferred to transoral rigid endoscopy as it allows for a greater range of voicing options and visualization of velopharyngeal competency during the assessment [10]. A recent study revealed that 750,000 diagnostic laryngeal endoscopic evaluations are performed each year at an esti-

ated annual cost of \$225 million dollars [3].

Due to the high cost and perceived discomfort associated with the diagnostic laryngeal endoscopic evaluation, it is prudent to consider less expensive and invasive options for assessment of potential laryngeal pathology. Current non-invasive assessment techniques that have been investigated include ultrasound and electroglottography (EGG). Ultrasound imaging uses sound waves to provide “pictures” of internal anatomy. Laryngeal ultrasound has been used to reliably identify the presence of vocal nodules in pediatric patients, but its ability to discriminate between different types of vocal fold pathologies has not been examined [11]. Additionally, ultrasound has been used to determine the presence of vocal fold paralysis following pediatric cardiovascular surgery, but with less specificity than the traditional diagnostic laryngeal endoscopic evaluation [9]. Electroglottography applies an imperceptible electrical current through localized tissues of the neck. It measures the degree of contact between the vocal folds. EGG signals are used to noninvasively characterize vocal fold dynamics [12, 13, 14] which are altered by the presence of vocal pathologies. This technique is being actively investigated to identify the signal features that can accurately and reliably detect vocal pathologies [15, 16]. While EGG approaches to pathology detection require vocal fold activity, another electrical current based technique is available that characterizes the passive properties of a biological tissue without requiring vocal fold activity. The passive electrical properties of a biological tissue, referred to as the tissue bioimpedance, are related to the underlying tissue physiology (e.g. fluid content, tissue type, cellular membrane health, tissue geometry). Tissue bioimpedance has recently been utilized in studies of neuromuscular disorders [17], skeletal muscle injuries [18], and swallowing [19, 20, 21].

A novel use for bioimpedance measures that has not yet been explored is its application for determining the health of vocal fold tissues by detecting vocal fold pathologies. The vocal folds are multilayered structures that consist of an outer epithelial layer, three connective tissue layers, and the vocalis portion of the thyroarytenoid muscle [22]. Each layer provides unique structural and

mechanical properties that are necessary for the characteristic vibration that produces human voicing. Vocal pathologies characteristically impact varying layers of the vocal folds. Even slight changes in the structure or viscoelastic properties of the vocal folds can cause significant disequilibrium into the delicate myoelastic aerodynamic balance responsible for normal voicing [23, 24]. Identifying the presence of these types of tissue changes in the vocal folds via non-invasive, economical, and readily accessible means would improve the timeliness of dysphonia diagnosis and decrease the time needed to achieve efficacious treatment. To evaluate if bioimpedance based analysis (using Cole-impedance modeling) may be a potential technique for diagnosis of vocal folds pathology, this research aims to first determine if vocal folds activity has a significant impact on localized neck tissue bioimpedance. Towards this aim, bioimpedance measurements were collected from a sample of non-dysphonic, healthy adults in four different vocal folds states (open, closed, voicing) to determine if there were statistically significant differences between states. The following sections detail the data collection methods, analysis approaches, overall study results, and discusses the results and their implications.

2. Material and Methods

2.1. Research Participants

This research was approved by The University of Alabama’s Institutional Review Board prior to participant recruitment and enrollment (UA IRB-19-04-2277). Adult participants were recruited through word of mouth and informational flyers. Interested individuals contacted the principle investigator to make an appointment for participation in the study. On the day of the appointment, the consent form was reviewed and signed by the participant. Data was collected from 10 young adults (22.1 ± 2.98 years of age, 3 women, 7 men) for this study.

85 2.2. Localized Bioimpedance Measurements

Bioimpedance measures are collected by applying an excitation current to biological tissue and measuring the voltage response ($Z = V/I$), at either a single or multiple frequencies. The use of multiple frequencies supports analysis of how different features (related to different underlying physiology features) are altered
90 as a result of tissue conditions. For example, low and high frequency measurements are often attributed to the extra-cellular and intra-cellular content and mid-band frequencies attributed to cellular membrane properties, tissue interconnections, and tissue type. For this reason, multi-frequency measurements are collected in this study because they may provide deeper insight into vocal
95 folds tissue properties than a single measurement.

Measurements from each participant were collected using a tetrapolar configuration of electrodes placed on the external skin surface proximal to the larynx of each participant. A tetrapolar configuration is utilized to reduce (but cannot remove) the effects of the electrode/tissue interface impedance which is typically
100 much larger than the tissue impedance. For further details regarding tetrapolar measurements, readers are recommended to review the works of Grimnes and Martinsen [25] and Aliau-Bonet and Pallas-Areny [26]. The larynx was identified through palpation and four adhesive electrodes were placed on either side of the laryngeal notch. The voltage sensing electrodes (V+, V-) were placed
105 approximately 2.5 cm from the larynx with the current injection electrodes (I+, I-) spaced approximately 3 cm (center-to-center) from the sensing pair. A sample of this configuration and the electrode placement on a study participant are detailed in Fig. 1. An ImpediMed SFB7, a portable bioimpedance device that measures discrete frequencies was the instrument utilized for participant mea-
110 surements. This instrument injected a small sinusoidal electrical current into the biological tissues of the larynx through the outer electrodes (I+, I- in Fig. 1) and measured the voltage response between the inner electrodes (V+, V- in Fig. 1) for the impedance calculation.

Bioimpedance measurements were collected from each participant under the
115 following 4 conditions:

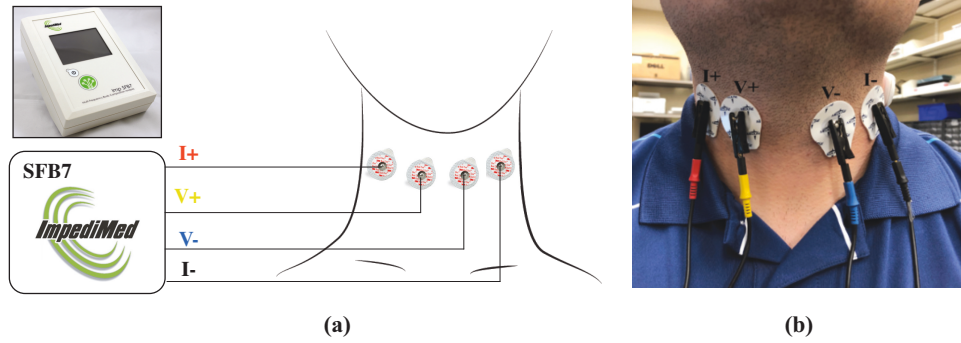


Figure 1: (a) Test setup to interface SFB7 to neck of study participants for measurement of tissue impedance proximal to larynx and (b) example of electrode placement on a single study participant.

- 1) Abduction. The participant was instructed to relax and breathe normally with the vocal folds in the abducted (open) position for ten seconds. A sample of the vocal folds in this position is given in Fig. 2(a).
- 2) Adduction. The participant was instructed to take a deep breath in, hold their breath, and to bear down on the sides of the chair they were sitting to close their vocal folds, for measurements in an adducted state. An image of vocal folds in this position (though not from a study participant, because the vocal folds were not visualized in this study) is given in Fig. 2(b). Participants held this position for five seconds. A limitation of this study is that the vocal folds were not visualized to confirm adducted state during measurement.
- 3,4) Voicing. The participant was instructed to hold out the vowel sounds “eee” (condition 3) and “ah” (condition 4) for 10 seconds and a 5 second voicing sample was extracted that excluded voicing onset and offset. Both of these voicing states require activity/vibration of the vocal folds altering the tissue geometry compared to the abducted and adducted states.

Participants were seated comfortably in a hard-back chair for the totality of data collection. At the conclusion of the study, the electrodes were removed,

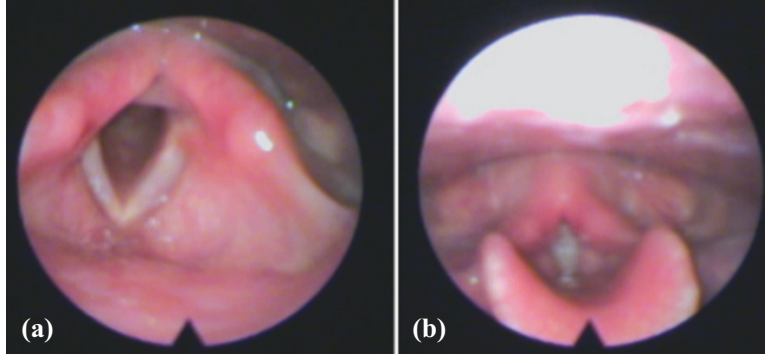


Figure 2: Example of vocal folds in the (a) abducted and (b) adducted states.

and the neck was cleaned of the adhesive material. The measurements were
 135 downloaded from the SFB7 instrument in their raw format for further import
 and post-processing in MATLAB.

2.3. Cole-impedance Model Parameter Identification

One method of bioimpedance analysis compares individual discrete frequen-
 cies of datasets for differences, but this approach is limited in that a single
 140 discrete frequency can be challenging to link to a specific physiological feature.
 Alternatively, analysis using electrical equivalent circuit models reduce a dataset
 with a large number of datapoints to a few circuit parameters that can be easily
 compared, with models selected to approximate the physiological of the tissue
 being measured. With vocal pathologies expected to impact cellular membrane
 145 properties of the vocal folds the analysis in this study will employ the equivalent
 circuit approach, to determine if the circuit parameters identified are sensitive
 to the changes in vocal folds state.

One widely utilized equivalent circuit model for this approach is the Cole-
 impedance model, introduced by Kenneth Cole in 1940 [27]. This model contains
 150 three electrical circuit components, two resistors (R_∞ , R_1) and one constant
 phase element (CPE). The units of a CPE are $\text{F} \cdot \text{sec}^{\alpha-1}$. The CPE has electrical
 characteristics that place it between a resistor ($\alpha = 0$) and an ideal capacitor
 ($\alpha = 1$). This electrical equivalent circuit model has been widely utilized to

represent the frequency-dependent electrical impedance of biological tissues [28]

155 and recently utilized in studies of localized tissues and their alterations as a result of exercise/activity [29, 30]; supporting its use to model the localized tissues in this work. The electrical impedance of the Cole-impedance model is expressed as:

$$Z = R_{\infty} + \frac{R_1}{1 + (j\omega)^{\alpha} R_1 C} = R + jX \quad (1)$$

where R and X represent the resistance and reactance (in Ohms), which are
160 often used to plot impedance datasets. The resistances in this model are often attributed to the tissue fluids with the CPE characteristics attributed to tissue type/structure.

The Cole impedance model parameters (R_{∞} , R_1 , C and α) were extracted from the datasets collected from each study participant. Extractions were done
165 by applying a particle swarm optimization (PSO) that minimized the squared difference (of the real and imaginary impedance components) between the experimental data (from 3 kHz to 280.6 kHz) and the Cole impedance model. Metaheuristic optimization procedures such as PSO have been previously utilized for estimating bioimpedance parameters from impedance datasets showing
170 accurate results [31]. Based on the high accuracy of previous PSO implementations and the ease of implementation using available MATLAB functions, this approach was adopted in this work. The objective function for the PSO optimization applied in this work is:

$$\min_x f_0(x) = \sum_{k=1}^n (\text{Re}\{Z_k(x) - y_k\})^2 + (\text{Im}\{Z_k(x) - y_k\})^2 \quad (2)$$

where $f_0(x)$ is the objective function, n is the number of discrete frequencies
175 used for fitting (200 in this study), y_k is the collected electrical impedance impedance at the k -th frequency, $Z_k(x)$ is the impedance of the Cole impedance model with x (the vector of the model parameters R_{∞} , R_1 , C , α), and Re and Im denote the real and imaginary components of the impedances. This procedure was implemented using the **particleswarm** function available in
180 MATLAB with the following options: *Swarm Size*= 1000, *Social Adjustment*

$Weight=1$, $MinNeighborsFraction=0.6$, and the hybrid functionality was enabled to apply the **fmincon** solver after the PSO solver terminated. Constraints were added with lower and upper boundaries for $[R_\infty, R_1, C, \alpha]$ fixed at $[1\text{ m}\Omega, 1\text{ m}\Omega, 1\text{ nF} \cdot \text{sec}^{\alpha-1}, 0.5]$ and $[100\text{ }\Omega, 100\text{ }\Omega, 0.1\text{ mF} \cdot \text{sec}^{\alpha-1}, 1.05]$, respectively.

2.4. Statistical Testing: Friedman Test

Statistical testing was applied to compare the Cole-impedance impedance parameters obtained from all 4 vocal folds test conditions, to test the null hypothesis that there are no differences between the parameters in each state. For this testing, the non-parametric Friedman test was applied to the organized datasets in SPSS Statistics 26. Statistical significance was accepted at the $p < 0.05$ level in this work.

3. Results

A sample of the complete set of impedance datasets (3 kHz to 1 MHz) collected from two of the participants, both men, are given in Figs. 3(a) and 4(a). In both Figs. 3 and 4 subplots (a), (b), and (c) visualize this data as a Nyquist, resistance/frequency, and reactance/frequency plots, respectively. The Nyquist plot is the conventional representation of bioimpedance datasets, but does not present details of the frequency dependence which is why (b) and (c) have been included. Each of the 4 vocal folds states that were measured are represented by different colors: adducted (black), abducted (red), voicing "ah" (blue), voicing "eeee" (green). Each line in subplots (a)-(c) represents one complete impedance sweep (with 5 collected/analyzed). The datasets from these two participants were selected because Fig. 3 represents a case with noticeable visual differences between states while Fig. 4 shows more significant overlap. Variations in the measured impedance are expected based on the instrument, participant movement, and breathing. For these reasons, the average of the set of reduced frequency measurements (3 kHz to 280 kHz to limit the influence of

high-frequency artifacts) for each vocal fold state were calculated. For reference,
 210 these averages are given in subplots (d), (e), and (f) as solid lines for the Nyquist,
 resistance/frequency, and reactance/frequency plots, respectively. These sets
 of averaged values more clearly visualizes the differences between each vocal
 fold state for both participants. Note that the reduced frequency datasets (3
 kHz to 280 kHz) are shown in subplots (b)-(e) in both Figs. 3 and 4 while
 215 subplot (a) shows the complete range (3 kHz to 1 MHz). The complete range is
 provided to highlight the high-frequency artifacts that can occur above 300 kHz.
 Those readers interested in further details of high-frequency artifacts/errors in
 bioimpedance measurements are directed to the work of Ayllon et. al [32].

Observing the average datasets, each exhibit decreasing resistances with in-
 220 creasing frequency for all states (most clearly shown in Figs. 3(e) and Figs. 4(e))
 and low/high frequency reactances that approach 0Ω with a mid-frequency min-
 ima occurring in the band from 10 kHz to 100 kHz (most clearly shown in Figs.
 3(f) and Figs. 4(f). This frequency-dependent behavior is well-represented by
 the Cole-impedance model. To highlight this simulations of (1) using the Cole-
 225 impedance model parameters determined by the PSO described in Sec. 2.3 are
 given in Figs. 3(d)-(f) and Figs. 4(d)-(f) as dashed lines. Both experimental
 (solid) and simulations (dashed) show very good visual agreement for each of
 the vocal fold states for both participants.

The complete range of Cole-impedance parameters (R_∞ , R_1 , C , α) identified
 230 by the PSO are given as boxplots in Fig. 5. In addition to these parameters, the
 theoretical frequency at which the reactance reaches its peak (f_p) was calculated
 using the Cole-impedance parameters using:

$$f_p = \frac{1}{2\pi(R_1 C)^{1/\alpha}} \quad (3)$$

Visually, the parameters R_∞ , R_1 , C , and f_p all have similar medians and ranges,
 with the parameter α showing the greatest differences across vocal folds states.
 235 Friedman tests were run to determine if there were differences in Cole-parameter
 values (and f_p) across the four different vocal folds states. While there were
 differences in the medians of each parameter (observed in Fig. 5) the differences

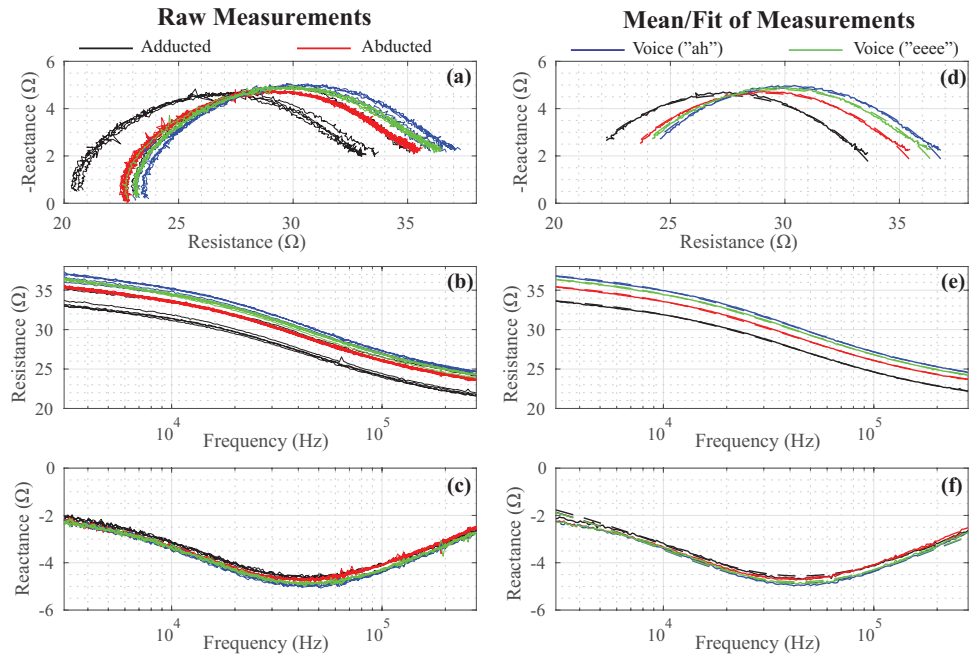


Figure 3: Raw bioimpedance measurements (a,b,c) collected from Participant 4 in the adducted (black), abducted (red), voicing "ah" (blue), and voicing "eee" (green) states and mean/simulations (using Cole-impedance parameters) of raw measurements (d,e,f).

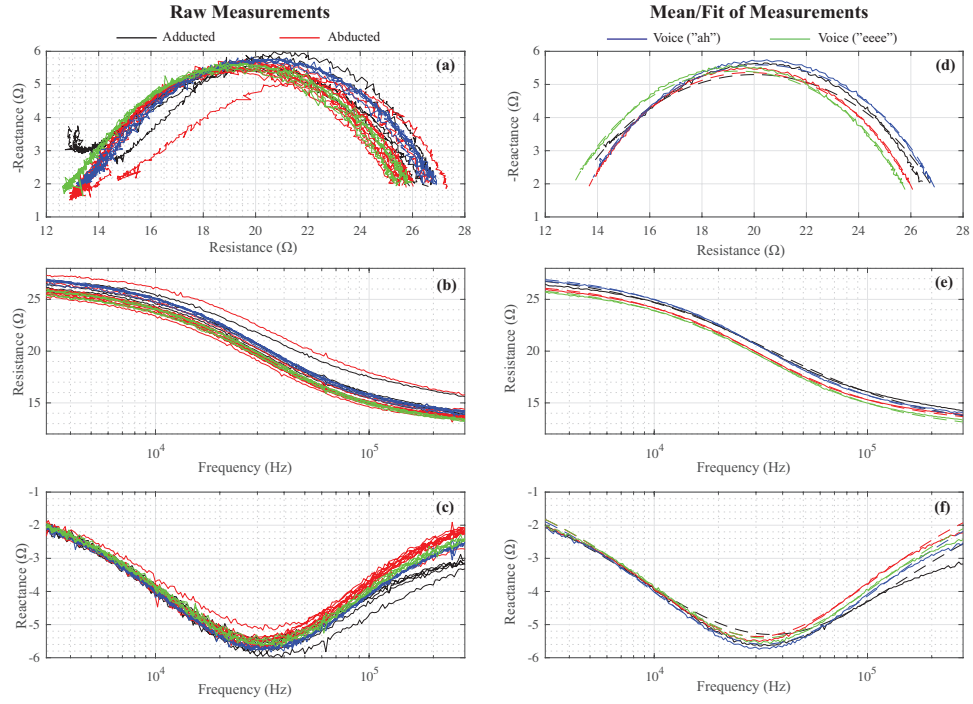


Figure 4: Raw bioimpedance measurements (a,b,c) collected from Participant 5 in the adducted (black), abducted (red), voicing "ah" (blue), and voicing "eee" (green) states and mean/simulations (using Cole-impedance parameters) of raw measurements (d,e,f).

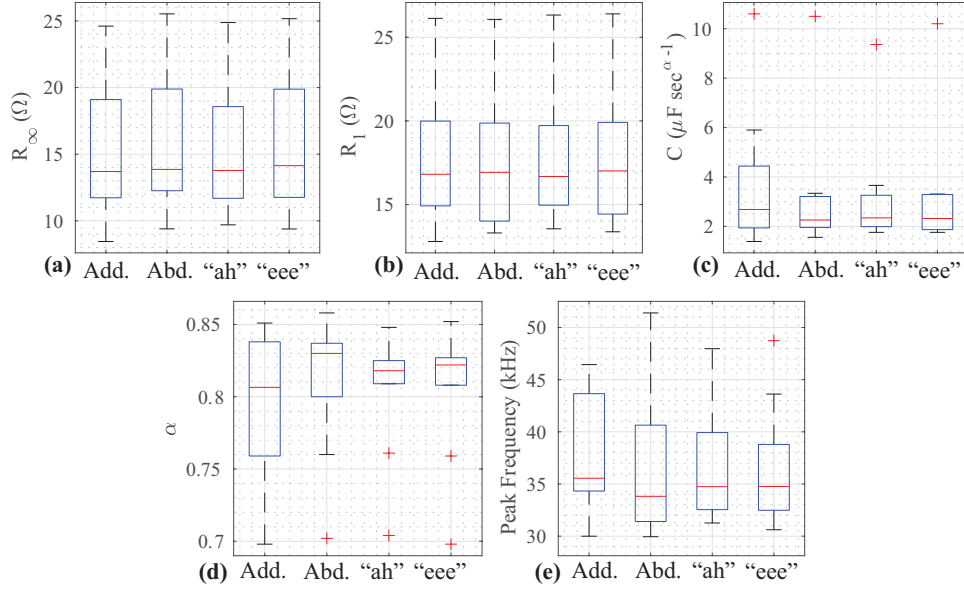


Figure 5: Summary of Cole-impedance parameters (R_∞ , R_1 , C , α) and peak frequency (f_p) determined from the localized tissues of study participants in each of the 4 vocal folds states. The red line of each box represents the median of the dataset, with the top and bottom of the box representing the 25th and 75th percentiles of the sample. The whiskers extend to the most extreme data points not considered outliers, and outliers (values more than $1.5x$ the interquartile range away from the bottom or top of the box) are plotted individually using the '+' symbol.

were not statistically significant ($R_\infty : \chi^2(3) = 5.04, p = 0.169$; $R_1 : \chi^2(3) = 4.40, p = 0.218$; $C : \chi^2(3) = 6.84, p = 0.077$; $\alpha : \chi^2(3) = 5.88, p = 0.118$, $f_p : \chi^2(3) = 6.84, p = 0.077$).

4. Discussion

The differences in vocal folds states/activity across the four cases (adducted, abducted, and voicing "ah"/"eee") for study participants did not result in statistically significant differences in the identified Cole-model parameters or peak frequency of the averaged localized bioimpedance datasets. While individual datasets did show variation across consecutive measurement of the same vocal folds positions (see Fig. 4), the averaging of multiple datasets is expected to be

a representative measure of the localized tissue properties that are not altered as a result of vocal folds activity or position. Averaging was adopted because
250 of the localized impedance changes that have been reported to occur during skeletal muscle contraction. As an example, Kitchen and Freeborn reported increases in bicep tissue resistance up to 6.75Ω during contractions [33] which can significantly impact stepped-sine bioimpedance measurements (which is the technique employed by the SFB7 utilized in this study) and their interpretation
255 (preventing fit with the Cole-impedance model). Skeletal muscle contraction was expected for participants who may have swallowed during the resting state, during voicing, and adduction, but the level of resistance changes is expected to be much less than the changes reported by Kitchen and Freeborn (which utilized an exercise stimulus to induce changes in a larger muscle group). Support for muscle contraction causing an increase in localized tissue impedance
260 of neck tissues is also observed in the reported impedances by Ward et. al [19] and Schultheiss et. al [21]. In both studies, increases in tissue resistance were observed prior to a decrease attributed to the transit of the fluid during the swallow. While Ward et. al reported that the anatomical or physiological correlates of this "hump" in the waveforms was unclear, it could be the initial contraction
265 of skeletal muscle prior to the movement of fluid during the swallow. This is supported by the results of Schultheiss et. al [21], which noted an increase in surface electromyography activity that roughly aligned with the initial increase in localized resistance.

270 The fact that there are no statistically significant differences in the identified Cole-model parameters of the averaged localized bioimpedance datasets is important because it supports that averaged localized bioimpedance measures of the neck/larynx may provide a non-invasive alternative to endoscopic visualization for vocal pathology identification and an alternative to EGG that does
275 not require phonation. Moving towards a technique that assesses the tissue properties directly and not only an effect (vocal fold contact area) of changes of the tissue properties. Additionally, the lack of statistically significant differences is clinically useful as it indicates that specific conditional factors (such

as voicing) are not necessary for accurate data collection with this technique.

280 This will expand the clinical utility of this technique by making it a viable assessment option for populations that are not able to follow directions and those that cannot tolerate laryngoscopic evaluation.

The application of EGG to assess vocal fold pathologies requires that vocal folds tissues have significant structural alterations that impact the contact area of these tissues during glottal activity. These changes in vocal fold contact area alter the impedance of the localized tissue which are reflected in the EGG waveform [34]. However, as noted by Hampala et. al the vocal fold contact area is not the only source of impedance change. Sources of change can include mucus bridges between vocal folds, uneven distributions liquid (influencing tissue conductivity), and non-uniform vocal folds tissue properties [34].
290 Additionally, differences in the execution of the glottal activity may also alter the EGG waveform and its interpretation.

While localized bioimpedance measurements will be altered by the same factors that include EGG waveforms (fluid distributions, non-uniform tissue properties) there is still strong support for their investigation for vocal fold pathology. Specifically, using multi-frequency measurements and Cole-modeling may support differentiation of the sources contributing to the impedance. Recently, Fu and Freeborn investigated the localized bioimpedance alterations (and subsequent Cole-model alterations) from activity of the biceps [29, 30]. They
300 reported statistically significant differences in R_∞ and R_1 after concentric activity (attributed to fluid shifts in the tissue) but not changes in C or α [29]. In an additional study utilizing eccentric activity as the exercise stimulus, statistically significant changes in C were reported in the days following activity. These alterations were attributed to the expected muscle damage from the eccentric stimulus and aligned with periods of swelling of the tissue [30]. Therefore, it
305 may be possible to differentiate vocal folds pathologies that alter tissue properties using the CPE parameters (C and α) of the Cole-model. This supports that further effort is warranted to investigate this model and relations to tissue alterations from pathology, injury, and damage. However, this requires further

310 research with measurements from both healthy and pathologic populations and cannot be answered with the results of the current study (which only collected measurements from a healthy, adult population). In fact, a limitation of the current study is that the bioimpedance measurements were collected from a small group ($N = 10$) with homogeneous age (22.1 ± 2.98 years). Further studies are necessary to evaluate if the results of this study are reproducible across 315 populations with varying age and body composition.

Of significant interest to clinical practice is the indication that the bioimpedance measures are not being sensitive to changes in vocal fold activity. This could eliminate the need for phonation during clinical assessment if bioimpedance features (such as C of the Cole-impedance model parameters) are determined to be 320 reliable biomarkers of vocal fold pathology. This is expected to help screening by reducing the overall activities during clinical assessment, which should improve patient compliance during this assessment. It is expected that collecting bioimpedance measurements while a patient is sitting and breathing normally 325 will be less time- and training intensive than collecting measurements during phonation. These challenges are expected to be most significant in pediatric populations and adult populations with significant neurologic impairment.

While the use of the Cole-impedance model to represent bioimpedance datasets in this work continues to support the use of this model, it is important to highlight it is not the only possible equivalent circuit model to represent bioimpedance 330 [28]. An important underlying question that still remains to be resolved is the strength of associations of the Cole-impedance model parameters (R_∞ , R_1 , C , α) and the underlying physiological features of the tissue. That is, while R_∞ and R_1 are often attributed to tissue fluid and the CPE to cellular membrane properties further study is still necessary to validate. This validation is an important 335 step to improve understanding and interpretation of impedance measurements for both basic research and clinical application.

5. Conclusion

This study evaluated the localized bioimpedance of the neck/laryngeal tissues of healthy, young adults during four different vocal folds states (adducted, abducted, voicing). While the tissue bioimpedance in each state did show variation across multiple consecutive measurements, the averaged datasets reduced to their equivalent Cole-impedance model representations $((R_\infty, R_1, C, \alpha))$ did not have statistically significant differences. These results support that the averaged electrical tissue properties may not be sensitive to the variations that results from vocal folds activity. Therefore, localized tissue bioimpedance may be an alternative technique to assess vocal fold tissue health that does not require phonation during assessment, but this requires further study.

6. Acknowledgements

The authors would like to thank Alexis Ramirez and his support of the data collection in this study during his participation in a National Science Foundation funded Research Experiences for Undergraduates site at the University of Alabama. This material is based upon work partially supported by the National Science Foundation under Grant No. 1852161. Any opinions, findings, and conclusions or recommendations expressed in this material are those of the author(s) and do not necessarily reflect the views of the National Science Foundation.

References

- [1] S. R. Schwartz, S. M. Cohen, S. H. Dailey, R. M. Rosenfeld, E. S. Deutsch, M. B. Gillespie, E. Granieri, E. R. Hapner, C. E. Kimball, H. J. Krouse, J. S. McMurray, S. Medina, K. O'Brien, D. R. Ouellette, B. J. Messinger-Rapport, R. J. Stachler, S. Strode, D. M. Thompson, J. C. Stemple, J. P. Willging, T. Cowley, S. McCoy, P. G. Bernad, M. M. Patel, Clinical practice guideline: Hoarseness (dysphonia), Otolaryngology–Head and Neck Surgery 141 (1_suppl) (2009) 1–31. doi:10.1016/j.otohns.2009.06.744.

- [2] R. J. Stachler, D. O. Francis, S. R. Schwartz, C. C. Damask, G. P. Digoy, H. J. Krouse, S. J. McCoy, D. R. Ouellette, R. R. Patel, C. C. W. Reavis, L. J. Smith, M. Smith, S. W. Strode, P. Woo, L. C. Nnacheta, Clinical practice guideline: Hoarseness (dysphonia) (update), *Otolaryngology–Head and Neck Surgery* 158 (1-suppl) (2018) S1–S42. doi:10.1177/0194599817751030.
- [3] M. Benninger, C. Holy, P. Bryson, C. Milstein, Prevalence and occupation of patients presenting with dysphonia in the united states, *J. Voice* 31 (5) (2017) 594–600. doi:10.1016/j.jvoice.2017.01.011.
- [4] S. M. Cohen, J. Kim, N. Roy, C. Asche, M. Courey, Prevalence and causes of dysphonia in a large treatment-seeking population, *The Laryngoscope* 122 (2) (2012) 343–348. doi:https://doi.org/10.1002/lary.22426.
- [5] R. Martins, do Amaral H.A., E. Tavares, M. Martins, T. Goncalves, N. Dias, Voice disorders: etiology and diagnosis, *J. Voice* 30 (6) (2015) 761.e1–761.e9. doi:10.1016/j.jvoice.2015.09.017.
- [6] C. Rosen, T. Murry, Diagnostic laryngeal endoscopy, *Otolaryngologic Clinics of North America* 33 (4) (2000) 751–757.
- [7] V. Singh, M. Brockbank, G. Todd, Flexible transnasal endoscopy: is local anaesthetic necessary?, *J. Laryngology Otology* 111 (7) (1997) 616–618.
- [8] J. Ongkasuwan, K. Yung, M. Courey, The physiologic impact of transnasal flexible endoscopy, *Laryngoscope* 122 (6) (2012) 1331–1334.
- [9] J. Ongkasuwan, E. Ocampo, B. Tran, Laryngeal ultrasound and vocal fold movement in the pediatric cardiovascular intensive care unit, *Laryngoscope* 127 (1) (2017) 167–172.
- [10] C. Milstein, S. Charbel, D. Hicks, T. Abelson, J. Richter, M. Vaezi, Prevalence of laryngeal irritation signs associated with reflux in asymptomatic volunteers: impact of endoscopic technique (rigid vs. flexible laryngoscope), *Laryngoscope* 115 (12) (2005) 2256–2261.

- [11] J. Ongkasuwan, D. Devore, S. Hollas, J. Jones, B. Tran, Laryngeal ultrasound and pediatric vocal fold nodules, *Laryngoscope* 127 (3) (2017) 676–678.
- [12] R. Baken, *Electroglottography*, *J. Voice* 6 (2) (1992) 98–110.
- [13] C. Herbst, W. Fitch, J. Svec, Electroglottographic wavegrams: a technique for visualizing vocal fold dynamics noninvasively, *J. Acoust Soc Am.* 128 (5) (2010) 3070–3078.
- [14] C. Herbst, *Electroglottography - an update*, *J. Voice* 34 (4) (2020) 503–526.
- [15] S. Sunil Kumar, T. Mandal, K. Sreenivasa Rao, Robust glottal activity detection using the phase of an electroglottographic signal, *Biomedical Signal Processing and Control* 36 (2017) 27 – 38. doi:<https://doi.org/10.1016/j.bspc.2017.03.007>.
- [16] A. Macerata, A. Nacci, M. Manti, M. Cianchetti, J. Matteucci, S. Romeo, B. Fattori, S. Berrettini, C. Laschi, F. Ursino, Evaluation of the electroglottographic signal variability by amplitude-speed combined analysis, *Biomedical Signal Processing and Control* 37 (2017) 61–68. doi:[10.1016/j.bspc.2016.10.003](https://doi.org/10.1016/j.bspc.2016.10.003).
- [17] J. Li, M. Jafarpoor, M. Bouxsein, S. Rutkove, Distinguishing neuromuscular disorders based on the passive electrical material properties of muscle, *Muscle Nerve* 51 (1) (2015) 49–55. doi:[10.1002/mus.24270](https://doi.org/10.1002/mus.24270).
- [18] L. Nescolarde, J. Yanguas, H. Lukaski, X. Alomar, J. Rosell-Ferrer, G. Rodas, Effects of muscle injury severity on localized bioimpedance measurements, *Physiol. Meas.* 36 (1) (2015) 27–42. doi:[10.1088/0967-3334/36/1/27](https://doi.org/10.1088/0967-3334/36/1/27).
- [19] L. Ward, W. McCullagh, J. Cichero, The use of bioimpedance analysis for the study of dysphagia, in: H. Scharfetter, R. Merwa (Eds.), 13th International Conference on Electrical Bioimpedance and the 8th Conference

on Electrical Impedance Tomography, Springer Berlin Heidelberg, Berlin, Heidelberg, 2007, pp. 683–686.

- [20] C. Schultheiss, T. Schauer, H. Nahrstaedt, R. Seidl, Evaluation of an emg bioimpedance measurement system for recording and analysing the pharyngeal phase of swallowing, *Eur Arch Otorhinolaryngol* 270 (2013) 2149–2156. doi:10.1007/s00405-013-2406-3.
- [21] C. Schultheiss, T. Schauer, H. Nahrstaedt, R. Seidl, Automated detection and evaluation of swallowing using a combined eim/bioimpedance measurement system, *Scientific World J.* 2014 (2014) Article ID 405471. doi:10.1155/2014/405471.
- [22] J. Kahane, The vocal folds and vocal fold vibratory patterns, *Otolaryngology—Head and Neck Surgery* 3 (1986) 1759–1766.
- [23] M. Hirano, S. Kurita, S. Sakaguchi, Ageing of the vibratory tissue of human vocal folds, *Acta oto-laryngologica* 107 (5-6) (1989) 428–433.
- [24] T. Hsiao, C. Wang, C. Chen, F. Hsieh, Y. Shau, Elasticity of human vocal folds measured in vivo using color doppler imaging, *Ultrasound in medicine & biology* 28 (9) (2002) 1145–1152.
- [25] S. Grimnes, O. Martinsen, Journal of physics d: Applied physics sources of error in tetrapolar impedance measurements on biomaterials and other ionic conductors, *J. Physics D: Appl. Physics* 20 (2006) 9–14.
- [26] C. Aliau-Bonet, R. Pallas-Areny, On the effect of body capacitance to ground in tetrapolar bioimpedance measurements, *IEEE Trans. Biomed. Eng.* 59 (12) (2012) 3405–3411.
- [27] K. Cole, Permeability and impermeability of cell membranes for ions, *Cold Spring Harbor Symp. Quant. Biol.* 8 (1940) 110–122.
- [28] T. Freeborn, A survey of fractional-order circuit models for biology and biomedicine, *IEEE J. Emerging Sel. Top. Circuits Syst.* 3 (3) (2013) 416–424. doi:10.1109/JETCAS.2013.2265797.

- [29] T. Freeborn, B. Fu, Fatigue-induced cole electrical impedance model
450 changes of biceps tissue bioimpedance, *Fractal Fract.* 2 (4) (27) 4. doi:
10.3390/fractalfract2040027.
- [30] B. Fu, T. Freeborn, Cole-impedance parameters representing biceps tissue
bioimpedance in healthy adults and their alterations following eccentric
exercise, *J. Adv. Res* 25 (2020) 285–293. doi:10.1016/j.jare.2020.05.
455 016.
- [31] D. Yousri, A. AbdelAty, L. Said, A. AboBakr, A. Radwan, Biological in-
spired optimization algorithms for cole-impedance parameters identifica-
tion, *Int. J. Electronics Commune.* 78 (2017) 79–89.
- [32] D. Ayllon, R. Gil-Pita, F. Seoane, Detection and classification of measure-
460 ment errors in bioimpedance spectroscopy, *PLoS ONE* 11 (6) (2016) 1–19.
doi:10.1371/journal.pone.0156522.
- [33] N. M. Kitchen, T. J. Freeborn, Contraction artifacts on biceps tissue
bioimpedance collected using stepped-sine excitations, in: *IEEE Southeast-
con*, 2019, pp. 1–6. doi:10.1109/SoutheastCon42311.2019.9020411.
- [34] V. Hampala, M. Garcia, J. Svec, R. Scherer, C. Herbst, Relationship be-
465 tween the electroglottographic signal and vocal fold contact area, *J. Voice*
30 (2) (2016) 161–171. doi:10.1016/j.jvoice.2015.03.018.